

TWO DIMENSIONAL NUMERICAL MODELS OF HOLLOW FIBER MEMBRANE CONTACTOR

N. Aryanti^{*)}, Y. Bindar^{**)} and I G. Wenten^{**)}

Abstract

Membrane contactor is separation processing unit using membrane as a contacting device. The major advantage of membrane contactor relies on its high contact area compared to conventional scrubber. One of the important applications of membrane contactor is to reduce emission of acid gases. In this work, modeling of membrane contactor is conducted to describe concentration distribution along fiber length used to predict effective fiber length by solving mass conservation equation. Solving of mass conservation equation requires information of fluid flow distribution obtained by solving continuity and momentum equations simultaneously. The finite volume method is used to obtain the solution. Modeling of fluid flow was carried out by adding Darcy's and Brinkman-Darcy flow models into Navier-Stokes equation. The momentum and continuity equations are solved for two-dimensional cylindrical coordinate. The results of velocity profile at axial direction were validated with Pangrle et. al. (1992) experimental data. The comparison shows that consideration using Brinkman-Darcy flow model give a good agreement with experimental data in which maximal axial velocity achieved is 0.047 m/s for this model and 0.05 m/s for experimental data. The concentration profiles at radial direction using Darcy and Brinkman-Darcy flow models have also been investigated. Furthermore, concentration profiles at axial direction using both the two flow models indicate a decrease of concentration along fiber length. The comparison between models and experimental data by Subhakti and Azmier (1997) agree very closely to the Brinkman-Darcy flow model. The prediction of effective fiber length was conducted based on minimum economical flux of membrane contactor. The calculation gives the effective fiber length obtained is 0.19 m at gas concentration, gas flow rate, and sorbent concentration of 0.02 mol/L, 0.8 m/s and 0.256 M respectively.

Key words: modeling, membrane contactor, Darcy, Brinkman-Darcy

Introduction

Membrane contactor is a separation processing unit using membrane as the contacting device. This paper concerns with gas-liquid membrane contactor for SO₂ gas cleaning. Sulfur dioxide is generally removed at the end of line scrubbing of the flue gas by an alkaline liquid or slurry. The removed SO₂ can be converted into waste product or into saleable byproducts such as gypsum and sulfuric acid. The majority commercial processes used are The Citrate, The Magnesium Oxide and The Wellman-Lord processes (Roberts and Friendlander, 1980). The conventional scrubbing processes are characterized by huge space requirements and related to high capital costs. Further, the conventional wet scrubbing processes suffer from number of deficiencies such as loading, flooding and entrainment limitation.

Membrane based processes are options rapidly gaining recognition as efficient, energy saving, and compact separation technologies. Hence, membrane-based processes for flue gas leaning could be an attractive alternative to replace conventional processes. The previous researchers have used membrane contactor in removal of volatile solute from solution (Yang and Cussler, 1985), absorption of CO₂

(Kreulan et. al., 1993; Rangwala, 1996; Iversen et. al., 1997).

In order to understand the phenomena occurs inside the membrane, microscopic observation is required. However, microscopic observation is difficult to conduct and require sophisticated instrumentations. Considering these limitations, modeling for the membrane contactor is necessary. Several researchers have conducted the membrane contactor modeling (Kreulan et. al., 1993; Podar et. al., 1996; Qin and Cabral, 1997; Roger and Long, 1997; Kaldis et. al., 1998; Viegas et. al., 1998; Coker et. al., 1998). However, the membrane contactor modeling is limited only for mass transfer and one-dimensional distribution models of flow and concentration.

Gas-Liquid Membrane Contactor

In a gas-liquid contactor, one phase is a gas or a vapor and the other phase is a liquid. The gas-liquid membrane contactor is further divided into a process where a gas or a vapor is transferred from the gas phase to a liquid phase and a process where a gas or a vapor is transferred from the liquid phase to the gas phase. In general, porous membranes are used for membrane contactors in which the membrane primarily acts as a barrier between the phases. Now,

^{*)} Dept. of Chemical Engineering, Diponegoro University, Semarang 50239

^{**)} Dept. of Chemical Engineering, Institut Teknologi Bandung, Bandung 40132

two concepts are possible, where the pores are filled either with gas phase or with the liquid phase. If a hydrophobic membrane is used such as poly tetrafluoroethylene, polyethylene and polypropylene, the aqueous solutions as the liquid phase does not wet the membrane and pores are filled with the gas phase (Non-wetted membrane). On the other hand, if a hydrophilic membrane is used, the aqueous phase will wet the membrane, i.e. wetted membrane (Mulder, 1996).

Membrane and sorbent selections are the major consideration in order to design membrane contactor. In this research, Sodium sulfite used for Wellman-Lord process and a polypropylene membrane is chosen. Membrane contactor must have a good membrane transfer and stability (includes thermal, chemical, wettability and mechanical) properties. Based on this thermal and chemical consideration, the polypropylene is used.

Modeling of Hollow Fiber Membrane Contactor

The mass transfer in membrane contactor is analyzed in terms of the mass transfer steps that occur. A specie of SO₂ gas phase must pass from the bulk to the gas liquid interface, membrane phase, dissolve and then probably react with some component from the liquid phase in a reaction zone. The dissolved gas and/or reaction products must then be transferred from the reaction zone to the bulk of the liquid. The mass transfer mechanism will effect on concentration distribution and flux profile along fiber length.

In this work, modeling of membrane contactor is conducted to describe concentration distribution along fiber length by solving mass conservation equation. Solving of mass conservation equation requires information of fluid flow distribution obtained by solving continuity and momentum equations simultaneously. The equation (1) to equation (3) present the continuity and momentum equations.

$$\frac{1}{\varepsilon} \frac{\partial}{\partial z} (\rho u) + \frac{1}{\varepsilon} \frac{\partial}{\partial r} (\rho v r) = 0 \quad (1)$$

$$\begin{aligned} & \frac{1}{\varepsilon} \frac{\partial}{\partial z} (\rho u u) + \frac{1}{\varepsilon} \frac{\partial}{\partial r} (\rho v u) \\ & = -\frac{\partial P}{\partial z} + \frac{1}{\varepsilon} \frac{\partial}{\partial z} \left(\mu \frac{\partial u}{\partial z} \right) + \frac{1}{\varepsilon} \frac{\partial}{\partial r} \left(r \mu \frac{\partial}{\partial r} \right) \\ & \quad + \rho g_z + S_i \end{aligned} \quad (2)$$

$$\begin{aligned} & \frac{1}{\varepsilon} \frac{\partial}{\partial z} (\rho u v) + \frac{1}{\varepsilon} \frac{\partial}{\partial r} (\rho v v) \\ & = -\frac{\partial P}{\partial z} + \frac{1}{\varepsilon} \frac{\partial}{\partial z} \left(\mu \frac{\partial v}{\partial z} \right) + \frac{1}{\varepsilon} \frac{\partial}{\partial r} \left(\frac{\mu}{r} \frac{\partial}{\partial r} (r v) \right) \\ & \quad + \rho g \end{aligned} \quad (3)$$

A hollow fiber is constituted by a cylindrical free space (lumen side) and a porous wall having

certain thickness. The fluid flows inside the lumen. The sulfur dioxide in the fluid diffuses into the porous wall due to the concentration difference.

The mass transfer of Sulfur dioxide is governed by a convection-diffusion equation from the lumen side through the porous membrane. The Sulfur dioxide reacts with sorbent instantaneously at outside boundary of the porous wall. The liquid mass components do not penetrate the pores wall because of the hydrophobic characteristic of membranes.

The equations to predict concentration distribution are based on cylindrical coordinate. They are the mass conservation equations for axial and radial direction (two-dimensional). The general mass conservation equation for A component is written below.

$$\begin{aligned} V \frac{\partial C_A}{\partial r} + U \frac{\partial C_A}{\partial z} &= \frac{1}{r} \frac{\partial}{\partial r} \left(r D \frac{\partial C_A}{\partial r} \right) \\ &+ \frac{\partial}{\partial z} \left(D \frac{\partial C_A}{\partial z} \right) + S \end{aligned} \quad (4)$$

The convection-diffusion equations above can be further developed to the forms of specific models. The term of S in that equation indicates the source term. The source term exists due to the change of concentration in the lumen and porous side. S terms in convection-diffusion equation are mathematical models for mass transfer mechanisms in a hollow fiber.

In order to simplify the prediction of concentration profile, both porous and lumen side has a model equation that only valid for each side. The mass transfer characteristics of membrane contactor follows the ordinary molecular diffusion for lumen side and Knudsen diffusion mechanism for porous side. The model in porous side follows the Porous Medium Model, which is well described by Darcy and Brikman-Darcy flow models. Based on this, the models further consider the mechanisms in the term of source term as can be shown in equation (5) and (6) for lumen and porous side respectively.

$$\begin{aligned} V \frac{\partial C_A}{\partial r} + U \frac{\partial C_A}{\partial z} &= \frac{1}{r} \frac{\partial}{\partial r} \left(r D \frac{\partial C_A}{\partial r} \right) \\ &+ \frac{\partial}{\partial z} \left(D \frac{\partial C_A}{\partial z} \right) + (k_g C_A R T) \end{aligned} \quad (5)$$

$$\begin{aligned} & \frac{1}{\varepsilon} \left(V \frac{\partial C_A}{\partial r} + U \frac{\partial C_A}{\partial z} \right) \\ &= \frac{1}{\varepsilon} \frac{1}{r} \frac{\partial}{\partial r} \left(r D \frac{\partial C_A}{\partial r} \right) + \frac{1}{\varepsilon} \frac{\partial}{\partial z} \left(D \frac{\partial C_A}{\partial z} \right) \\ & \quad + (k_m C_A R T) \end{aligned} \quad (6)$$

Both of the equations are solved using these assumptions below:

- No chemical reaction inside fiber
- Laminar and single phase flow
- Incompressible and Newtonian fluid
- Steady state and isothermal
- Temperature and pressure is 25°C, 1 atm
- Instantaneous reaction in shell side

Table 1 shows the values of the transport properties, hollow fiber parameters, and initial concentrations. The diffusivity value for SO₂ in the gas phase was estimated using the Chapman-Enskog equation. The tortuosity is predicted using Mackie-Miers equation (Iversen et al., 1997). The Reynolds-Sherwood-Schmidt Number is employed to obtain mass transfer coefficient at gas phase. The Knudsen-Ordinary Diffusion mechanism is applied to predict the mass transfer coefficient in the membrane.

Table 1. Summary of parameter used in this study

Diffusion of SO ₂ -N ₂	8.593. 10 ⁻⁶
Fiber Length	0.25 m
Shell Radius, R _s	0.01 m
Thickness	150 μm
Outside Fiber Radius	2.5 10 ⁻⁴ m
Number of fibers	100
Viscosity	1.38 10 ⁻³ kg.m.s ⁻¹
Density	2.28 kg/m ³
Tortuosity	3.42

Results and Discussions

Validation of velocity profile using experimental data

It is useful to briefly demonstrate the agreement of the model prediction with the experimental data. The measurement of velocity distribution is very difficult due to a micro size of the fiber diameter. However, an excellent attempt was conducted by Pangrle et al (1992) to measure the velocity profile inside the lumen using a Magnetic Resonance Imaging method. Their experimental data are used to be compared with the present prediction.

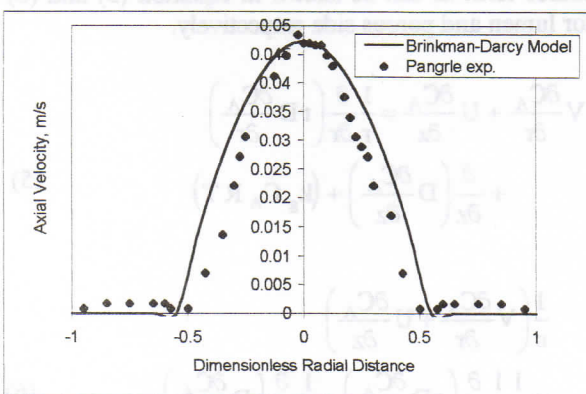


Figure 1 Comparison between experimental data and model using Brinkman-Darcy Equation

Figure 1 shows a good agreement between the data and the model at porous side. Both experimental data and model show similar fluid hydrodynamic

characteristic where maximum axial velocity is achieved at lumen side at the value of 0.048 m/s.

The effect of Fluid flow models on velocity profile

In order to explain the performance of the Darcy and Brinkman-Darcy flow models, both set of velocity profiles at axial and radial direction are compared in Fig 2, Fig.3 and Fig.4.

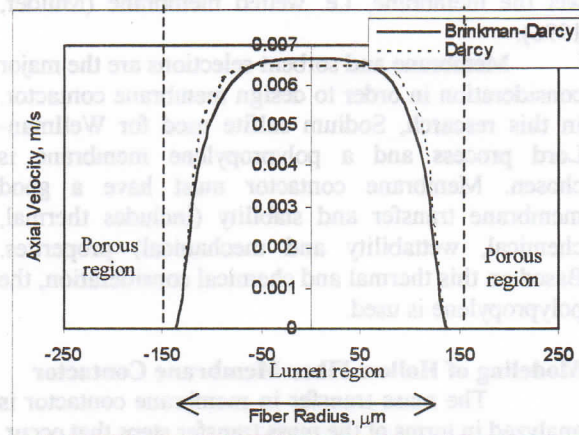


Figure 2 Comparison of predicted axial velocity profiles using Brinkman-Darcy and Darcy models at z = 0.25 m, U₀ = 0.008 m/s

Figure 2 presents the axial velocity profile for Darcy and Brinkman-Darcy flow models. This figure shows that the velocity decreases with the increase of fiber length. The decrease of axial velocity is related to drag force and reduction of gas component along the fiber length. The predictions of velocity using Darcy and Brinkman-Darcy models are not very much different each other. The values of axial velocity at porous region using Brinkman-Darcy is in the range of 10⁻⁹ m/s while using of Darcy is 10⁻⁷ m/s. In the porous side, the diffusion term plays a major role in the momentum transfer. In contrast, the velocity profile at lumen side is not significantly influenced by the diffusion term but by the convection term.

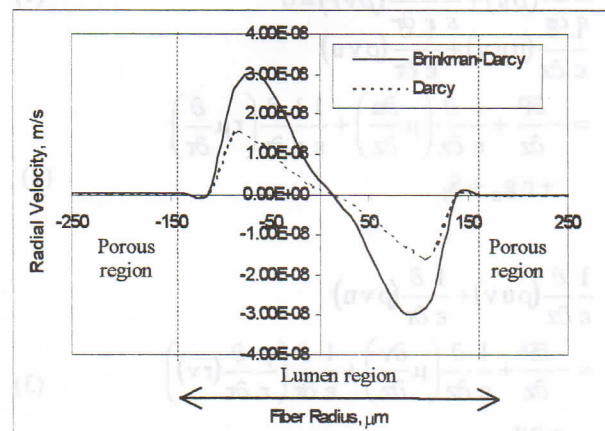


Figure 3 Comparison of predicted radial velocity profiles using Brinkman-Darcy and Darcy models at z = 0.25 m, U₀ = 0.008m/s

The radial velocity profiles using Brinkman-Darcy and Darcy models are significantly different at porous and lumen side, Fig 3. The Brinkman-darcy flow model exhibits higher values of radial velocity than Darcy model.

Both axial and radial velocity profiles result in similar characteristic at the porous and lumen side. In the porous region (up to fiber radius of $1.25 \cdot 10^{-4}$ m), the axial velocity profile does not appear because this velocity is very small comparing to that in the lumen side. Referring to Fig.2 and Fig.3, there is a significant difference in the velocity profiles at the lumen and porous side. The average axial and radial velocities in the porous side are in the ranges of 10^{-7} m/s and 10^{-12} m/s, and 10^{-3} m/s and 10^{-7} m/s respectively. This is due to a unique characteristics of the membrane contactor where the major parameter in the porous side dominated by the transport mechanisms, not by the convection flow, which is negligible.

The maximum and minimum velocity values located at $R = 0.5 R$ and $R = -0.5 R$, respectively, while very small values of the radial velocity occurs at porous side at $R = 0$ and $R = R$. Convection does not occur in radial direction. All of the movement in radial direction is due to diffusion momentum and mass transport.

Figure 4 presents the radial velocity profile as a function of the fiber length. Predicted radial velocity profiles along fiber length using Darcy and Brinkman-Darcy models can be compared each other.

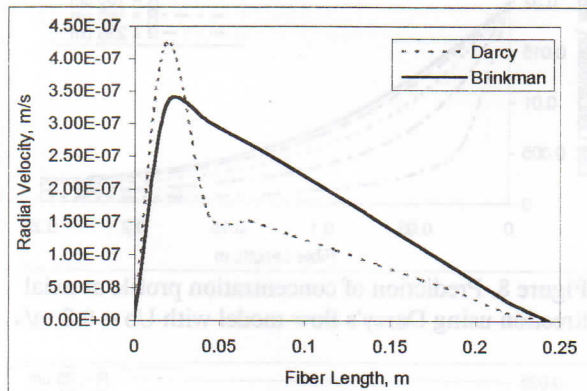


Figure 4 Comparison of predicted radial velocity profiles using Brinkman-Darcy and Darcy models at lumen side, $U_0 = 0.008$ m/s, $R = 35 \mu\text{m}$

Validation of concentration profile using experimental data

The predicted concentration distribution in the hollow fiber contactor results from the models can be expressed as a mass flux. In order to test the model, the predicted flux from both models is compared with the experimental data obtained from Subhakti and Azmier experimental (Azmier, 1997). They used a hollow fiber membrane contactor which have the

specification as listed in table 1. Gas and liquid sorbent used in their experiment was a gas mixture SO_2 in N_2 , and sodium sulfite.

The comparison of the experimental data and predicted results using various models are presented in Fig 5 as a function of gas velocity and flux of SO_2 .

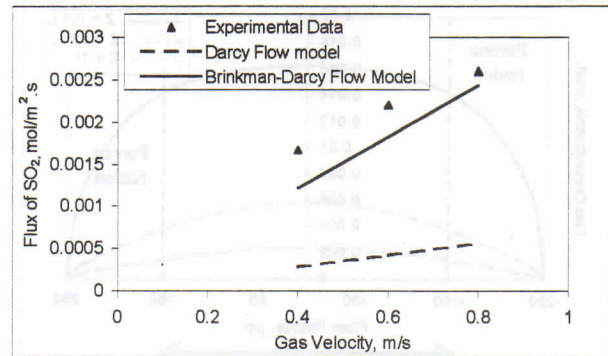


Figure 5 The comparison of model and experimental data for various gas velocity at lumen side, $z = 0.25$ m using sorbent concentration 0.256 mol/L

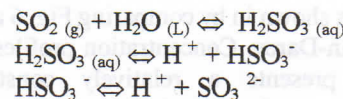
Figure 5 shows that the effect of gas to mass flux is clearly shown. This effect is similarly exhibited by the present prediction results using various models.

As shown in Figure 5, the predictions using Brinkman-Darcy model have a good agreement with experimental data. The diffusion in porous side dominates the mass transfer. Darcy's model results lower mass flux. This means that Brinkman-Darcy model works better than Darcy's.

All of the model development above is based on the resistance calculation that neglects mass transfer in the liquid phase. Based on Hikita et al. experimental (Hikita, 1977), the reaction rate constant of SO_2 and sodium sulfite is large. This leads that the assumption of the instantaneous reaction is quite valid. The calculation of the permeation flux is obtained by considering overall mass transfer coefficient which consists of gas resistance and membrane resistance only.

The model of mass transfer in the gas phase was used to calculate SO_2 concentration, which were completely determined by mass transfer from gas to membrane phase. The concentration at the gas-liquid interface, can be assumed to be zero (Kreulan, 1993) or non zero value from experimental data, such as data from Hikita et al (1977).

Chemical reactions are considered to be instantaneous reactions. Thus the reactions in the scrubbing solution occur as equilibrium reactions. The equilibrium reactions for SO_2 absorption into sulfite solutions are involve:



Concentration profiles in radial directions have never been reported by other researchers. The present models provide a computational mean to predict the concentration profiles radially and axially. The radial SO₂ profiles are presented in Fig. 6 and Fig. 7.

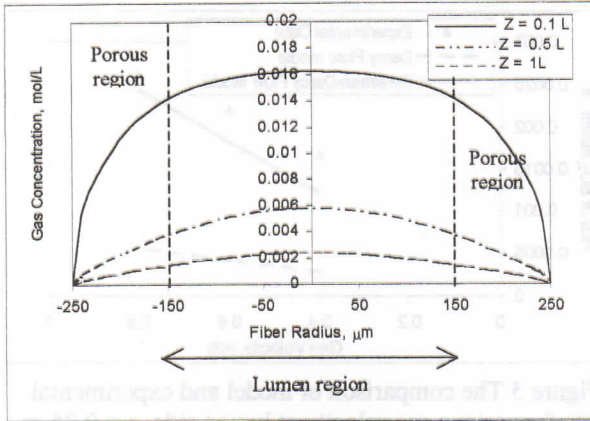


Figure 6. Prediction of concentration profile at radial direction using Darcy's flow model with $U_o = 0.8$ m/s

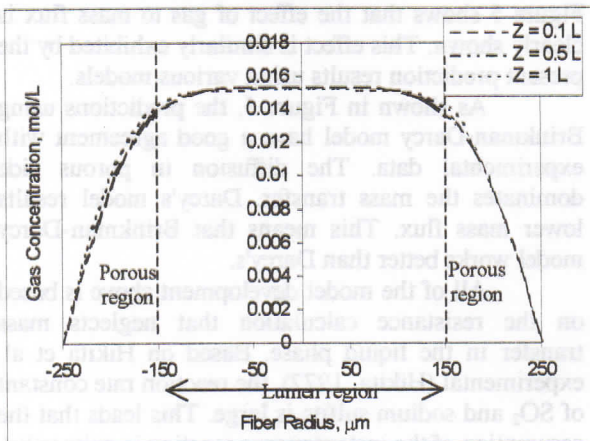


Figure 7. Prediction of concentration profile at radial direction using Brinkman-Darcy's flow model with $U_o = 0.8$ m/s

As shown in Fig. 6, concentration profiles at radial direction presents an increase of its value toward the center of lumen side. As it is expected, the concentration decreases along the fiber length. This is obvious since the phenomena is entirely governed by SO₂ transfer from the gas phase to the porous membrane along its length. The consideration means that the concentration distribution is dominated by convection in the lumen. The gas concentration decreases with increasing of fiber length because more SO₂ diffuse to the membrane inner face along the fiber length.

The effect of flow models, Darcy and Brinkman-Darcy, is shown in by comparing Fig. 6 and Fig. 7 for Brinkman-Darcy. Concentration profiles at radial direction presents a relatively constant concentration at lumen side and a sharp concentration

decrease at porous side. Furthermore, the figure also shows that the fiber length relatively did not influence on gas concentration. The phenomena is related to the values of gas velocity along the fiber length which it decrease with increasing of fiber length.

As shown in figure 7, the used of diffusion term $\mu \nabla^2 u'$ influence on the calculation of gas concentration. A sharp decrease of concentration in porous side is caused by gas diffusion through the pores. The calculation of concentration profile at porous side requires both membrane and gas mass transfer coefficients due to a serial of resistances against mass transfer in gas and membrane phase. In the gas filled pores mechanism, membrane mass transfer coefficient depends on the diffusion regime. Resistance to the transport comes from both the presence of a stagnant gas trapped within the membrane and the membrane structure. The resistance from stagnant gas is modeled by an ordinary molecular diffusion model. The influence of membrane structure is described by Knudsen diffusion. Hence, both diffusion mechanisms are used to predict mass transfer coefficient inside porous region. A sharp decrease of concentration in porous region is influenced by the membrane resistance. As a result, this dominates the concentration calculation.

Concentration profiles for axial direction are shown in Fig. 8 and Fig. 9 for Darcy and Brinkman-Darcy flow models respectively.

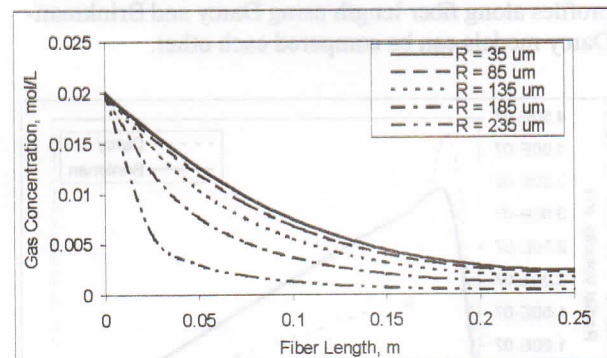


Figure 8. Prediction of concentration profile at axial direction using Darcy's flow model with $U_o = 0.8$ m/s

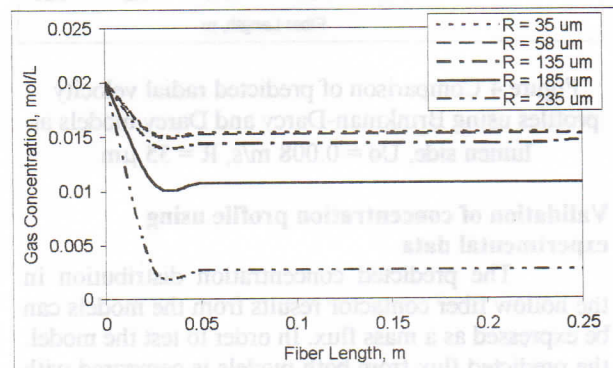


Figure 9. Prediction of concentration profile at axial direction using Brinkman-Darcy's flow model with $U_o = 0.8$ m/s

Both figures show a sharp decrease along fiber length. This is caused globally by the absorption process of SO_2 by Sodium sulfite liquid. SO_2 is always consumed by the reaction in the outer surface of porous region. This reduces the concentration of SO_2 in gas phase. In the case of gas inside fiber, chemical reaction does not occur inside the fiber due to the hydrophobic characteristic, membrane will be not wetted by sorbent consequently moreover SO_2 gas will fill membrane pores.

In figure 8 for Darcy flow model, the concentration difference at porous and lumen side is not apparent since there is only a slight decrease of SO_2 concentration, Fig. 1. This is due to Darcy's model characteristic in which the influence of diffusion term is neglected.

As shown in figure 9, decreasing of gas concentration at porous to lumen side is relatively large. This condition is related to Figure 7, wherein at lumen to porous side a sharp decrease of concentration occurs. This phenomenon is described by the presence of the diffusion effect in the Brinkman-Darcy flow model. Furthermore, the diffusion effect dominates the mass transfer in pore side. Both Knudsen and ordinary molecular diffusions prevail only in the porous side.

Calculation of Effective Fiber Length

In order to reduce the capital cost, the volume absorption to be used must be minimized. It can be achieved by using fiber length as short as possible. The prediction of effective fiber length is based on a comparison between a conventional scrubber and a membrane contactor.

Experimental runs for comparing conventional scrubber and hollow fiber contactor were carried out by Azmier and Subhakti (Azmier, 1997). Generally, packed column as a conventional scrubber with the rate separation of SO_2 is 0.5 kg/s requires column with 3.105 m in diameter and 19.9 m in height. The membrane for experiments above was a hollow fiber type with porosity of 70% and diameter of 0.9 mm. The module length was 30 cm, which consists of 100 fibers. Using the same capacity of 0.5 kg/s, the comparison between both two contactors is presented in Table 2.

An effective fiber length is predicted by calculating the minimum flux in membrane contactor. This value is converted into a gas velocity. Furthermore, the gas velocity is taken as a minimum radial velocity. The effective fiber length is obtained by plotting this minimum gas velocity value against the fiber length.

The calculation of an effective fiber length is based on Table 2. The membrane contact area is 0.028 m^2 . The calculation of minimal flux results 0.37 mol/hr.m^2 . This figure is equal to $8.08 \cdot 10^{-8} \text{ m/s}$ as a radial velocity. Figure 5.10 presents a simulation result for the radial velocity along the fiber length in

the lumen side with 0.008 m/s initial gas velocity. The result for an effective fiber length Fig. 10 is 0.19 m .

Table 2 Analytical dimension of conventional scrubber and membrane based process

	Conventional scrubber	Hollow Fiber Contactor
Capacity	0.5 kg/s	0.5 kg/s
Flux	250 mol/hr.m ²	10 mol/hr.m ²
Contactor volume	151 m ³	5.6 m ³
	Conventional scrubber	Hollow Fiber Contactor
Capacity	0.5 kg/s	0.5 kg/s
Flux	250 mol/hr.m ²	10 mol/hr.m ²
Contactor volume	151 m ³	5.6 m ³

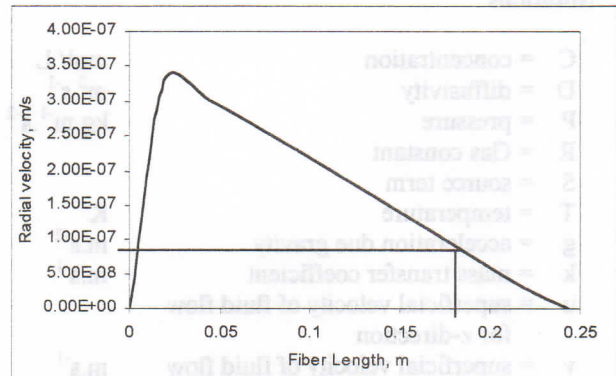


Figure 10 Profile of radial velocity at lumen side as a function of fiber length, $C=0.02 \text{ mol/L}$

Conclusion

The two-dimensional models of membrane contactor have been developed in order to describe fluid flow and concentration distribution, which is required for predicting effective fiber length. Model to predict fluid flow and concentration distribution is carried out for single fiber using two-dimensional cylindrical coordinate. Both fluid flow and concentration model follow the Porous Medium Model, in which the membrane thickness is considered as porous medium. Darcy and Brinkman-Darcy equation are applied for describing phenomena inside porous medium. In order to solve partial differential equation of momentum and mass transport simultaneously, the Finite Volume method is used.

The result of velocity profile at axial direction was validated with Pangrle et. al. (1992) experimental data. The comparison shows that consideration using Brinkman-Darcy equation results agree closely to experimental data in which maximal axial velocity achieved is 0.047 m/s for this model and 0.05 m/s for experimental data.

Concentration profiles have been presented by solving mass conservation equation using Darcy and Brinkman-Darcy consideration. The concentration profiles at axial direction using both two considerations indicate a decrease of concentration along fiber length. This profile will be related to calculation of effective fiber length. The simulation at different initial gas velocity has also been investigated and increasing of gas velocity achieves higher permeation flux. The comparison between models and experimental data by Subhakti and Azmier (1997) agree very closely to the Brinkman-Darcy porous model and Darcy lumen model.

The prediction of effective fiber length was conducted using minimum flux of membrane contactor. The calculation obtain the effective fiber length is 0.19 m at gas concentration, gas flow rate, and sorbent concentration 0.02 mol/L, 0.8 m/s and 0.256 M, respectively.

Notations

C = concentration	mol/ L
D = diffusivity	m ² .s ⁻¹
P = pressure	kg.m ⁻¹ .s ⁻²
R = Gas constant	
S = source term	
T = temperature	K
g = acceleration due gravity	m.s ⁻²
k = mass transfer coefficient	m.s ⁻¹
u = superficial velocity of fluid flow for z-direction	
v = superficial velocity of fluid flow for r-direction	m.s ⁻¹

Subscripts

g = gas
l = liquid
m = membrane
z = z-direction
r = r-direction

Greeks

ε = porosity	
ρ = density	kg.m ⁻³
μ = viscosity	kg.m.s ⁻¹

References

Azmier, I., and I K. P. Subhakti, 1997, "Development of Membrane Based Process for Flue Gas Cleaning" (in Indonesian), Research Report, ITB, p. 35-40.

Coker, D.T., B.D. Freeman, and G.K. Fleming, 1998, "Modeling Multicomponent Gas Separation Using Hollow Fiber Membrane Contactors", *AIChE J.*, 44(6), p.1289-1302

H. Kruelan et.al., 1993, "Microporous Hollow Fiber Membrane Module as Gas-Liquid Contactors. Part 2. Mass Transfer With Chemical Reaction", *J.Membrane Sci.*, 78, 217-238

Hikita, H., S. Asai, and T. Tsuji, 1977, "Absorption of Sulfur dioxide into aqueous Sodium Hydroxide and Sodium Sulfite Solutions", *AIChE*, 23(4), p. 538-544.

Iversen, S.B., V.K. Bhatia, K. Dam-Johansen, and G. Jonsson, 1997, "Characterization of Microporous Membranes for Use in Membrane Contactors", *J. Membrane. Sci.*, 130, p. 205-217

Kaldis, S.P., G.C. Kapantaidakis, T.I. Papadopoulos, and G.P.Sakelaropoulos, 1998, "Simulation of Binary Gas Separation in Hollow Fiber Asymmetric Membranes by Orthogonal Collocation", *J. Membrane. Sci.*, 142, p.43-59

Kreulan, H., C.A. Smolders, G.F. Versteeg and W.P.M. Van Swaaij, 1993, "Microporous Hollow Fiber Module as Gas-Liquid Contactors: Part 1 Physical Mass transfer Processes", *J. Membrane. Sci.*, 78, p. 197-216.

Kreulan, H., C.A. Smolders, G.F. Versteeg and W.P.M. Van Swaaij, 1993, "Microporous Hollow Fiber Module as Gas-Liquid Contactors: Part 2 Mass Transfer with Chemical Reaction", *J. Membrane. Sci.*, 78, p. 217-238.

Labecki, M., J.M. Piret, and B.D. Bowen, 1995, "Analysis of Fluid Flow in Hollow Fiber Modules", *Chem. Engng. Sci.*, 50(21), p.3369-3384

Mulder, M., 1996, "Basic Principles of Membrane Technology", 2nd ed., Kluwer Academic Publisher, Netherlands.

Pangrle, B.J., E.G. Walsh, C. Moore and D. DiBiasio, 1992, "Magnetic Resonance Imaging of Laminar Flow in Porous Tube and Shell Systems", *Chem. Engng. Sci.*, 47(3), p. 517-526.

Patankar, S.V., (1980), "Numerical Heat Transfer and Fluid Flow", Hemisphere, New York

Poddar, T.K., S. Majumdar, and K.K. Sirkar, 1996, "Removal of VOCs from Air by Membrane Based Absorption and Stripping", *J. Membrane. Sci.*, 120, p. 221-237

Qin, Y. and J.M.S. Cabral, 1997, "Lumen Mass Transfer in Hollow Fiber Membrane Processes with Constant External Resistances", *AICHE*, 44(4), p. 1975-1988.

Qin, Y. and J.M.S. Cabral, 1998, "Lumen Mass Transfer in Hollow Fiber Membrane Processes with non Linear Boundary Conditions", *AICHE*, 44(4), p. 836-848.

Rangwala, H.A., 1996, "Absorption of Carbon Dioxide Into Aqueous Solutions Using Hollow Fiber Membrane Contactors", *J. Membrane Sci.*, 112, 229-240

Roberts, D.L., and S.K. Friendlander, 1980, "sulfur Dioxide Transport Through Aqueous Solutions: Part 1. Theory.", *AICHE J.*, 26(4), p.594-602.

Roberts, D.L., and S.K. Friendlander, 1980, "sulfur Dioxide Transport Through Aqueous Solutions: Part 1. Experimental Results and Comparison with Theory.", *AICHE J.*, 26(4), p.603-610.

Rogers, J.D., and R.L. Long, 1997, "Modeling Hollow Fiber Membrane Contactor Using Film Theory, Voronoi Tessellation and Facilitation Factors for Systems with Interface Reactions", *J. Membrane. Sci.*, 134, p. 1-17

Yang, M.C., and E.L. Cussler, 1986, "Designing Hollow Fiber Contactors", *AICHE J.*, 32(11), p.1910-1916

... (mirrored bleed-through text from the reverse side of the page)

... (mirrored bleed-through text from the reverse side of the page)